

## **SEISMIC ASSESSMENT OF MASONRY CROSS VAULTS THROUGH NON-LINEAR STATIC ANALYSES**

**M. Alforno<sup>1</sup>, A. Monaco<sup>1</sup>, F. Venuti<sup>1</sup> and C. Calderini<sup>2</sup>**

<sup>1</sup> Politecnico di Torino, Dept. of Architecture and Design  
Viale Mattioli 39, 10125 Torino - Italy  
M. Alforno: [marco.alforno@polito.it](mailto:marco.alforno@polito.it)  
A. Monaco: [alessia.monaco@polito.it](mailto:alessia.monaco@polito.it)  
F. Venuti: [fiammetta.venuti@polito.it](mailto:fiammetta.venuti@polito.it)

<sup>2</sup> University of Genoa, Dept. of Civil, Chemical and Environmental Engineering  
Via Montallegro 1, 16145, Genoa, Italy  
C. Calderini: [chiara.calderini@unige.it](mailto:chiara.calderini@unige.it)

---

### **Abstract**

*Masonry cross vaults are common structural elements in historical buildings. They are largely diffused in all European countries, including those characterized by higher levels of seismicity. Although they have been constructed for centuries, they represent some of the most vulnerable elements of traditional architecture, especially with reference to horizontal loads. The understanding of their behaviour under seismic loading and the definition of their safety are crucial aspects for the accurate assessment of the global health conditions of historical buildings. In the present work, masonry cross vaults are analysed through the Finite Element Method (FEM) and static non-linear analyses are performed considering the effect of different brick pattern.*

*A simplified micro-modelling approach is adopted for the generation of the FEM models and two different brick arrangements are considered, i.e., radial bricks and diagonal bricks, which are the most widespread in European cross vaults. Static non-linear analyses are performed by monotonically incrementing a lateral acceleration until collapse. Results are analysed in terms of maximum load factor, crack pattern and damage mechanisms. The analysis of the results shows that the masonry apparatus strongly influences the vault seismic response both in terms of stiffness and ductility as well as in terms of global capacity.*

**Keywords:** Cross vaults; Masonry apparatus; FEM model; Push-over analysis, Seismic behaviour.

---

## 1 INTRODUCTION

European historical masonry buildings are often characterized by the presence of vaulted structures of complex geometry and cross masonry vaults are among the most widespread types. They are largely diffused in all European countries, including those characterized by higher levels of seismicity. Although they have been constructed for centuries, they represent some of the most vulnerable elements of traditional architecture, especially with reference to horizontal loads when the construction site is characterized by high levels of seismicity. For this reason, the assessment of their behaviour under seismic loading, and consequently the definition of a safety level, is a crucial precondition for the accurate assessment of the global safety of historical buildings.

Compared to simple masonry walls, numerical modelling of masonry vaulted structures is particularly complex due to their three-dimensional curved geometry and articulated masonry pattern. As a matter of facts, vaults can be built according to different brick patterns, which, in historical building practices, were generally chosen for technical reasons.

In the present work, cross vaults of ideal geometry are modelled through the simplified micro-modelling approach in the framework of Finite Element Method (FEM) [1]. This modelling approach has already been used by the authors and successfully validated with physical in-scale models [2]. The use of micro-mechanical models allows to simulate block-to-block interactions and therefore the real interlocking of bricks. In this work, two different brick arrangements are considered, i.e., radial bricks and diagonal bricks, which are most found in European cross vaults. Static non-linear analyses are performed by monotonically incrementing a lateral acceleration until collapse. Results are analysed in terms of maximum load factor, crack pattern and damage mechanisms.

## 2 DESCRIPTION OF THE MODEL

In this section the main features of the FEM model are described in terms of geometry, mechanical parameters of materials and interface properties. Moreover, the load cases and the boundary conditions are illustrated.

### 2.1 Geometry and mechanical features

The geometry of the vault is obtained as intersection of two semi-circular barrel vaults. The base is squared with a net span of approximately 3.1 m and rise of 1.175 m. The volume is discretized into bricks of size 6x12x24 cm. The shape of the interlocked bricks along the diagonal arches is idealized and simplified. Four rigid corner supports are modelled at the base of the vault. Two different masonry apparatus are modelled, namely those which follow radial (R) and diagonal (D) path. More in detail, in the case of radial pattern, the longitudinal courses between bricks are disposed normal to the ring arches; conversely, in the case of diagonal pattern, the bed joints are oriented at a 45° angle. Figure 1 shows the details of the geometry and the discretization into bricks; as an example the vault with radial brick pattern is reported.

The discretization of the solid volume of the vault is conducted by means of a simplified micro-modelling approach which allows for the detailed definition of the brick pattern [1]. Such a method consists in the assemblage of a series of blocks connected with zero-thickness interfaces endowed with proper tangential and normal mechanical properties.

The mechanical properties of the blocks are defined through simple elastic behaviour, adopting the values suggested by [3] for historic brick-masonry. In particular, the density of the material  $\rho$  is assumed equal to 1800 kg/m<sup>3</sup> while the elastic modulus  $E$  and the Poisson's ratio  $\nu$  are equal to 1200 MPa and 0.2, respectively. The behaviour of the mortar joints is sim-

ulated through the insertion of an interaction property between all masonry surfaces into contact. The Authors have already validated this modelling approach in some previous research [2,4,5]. In the local tangential direction, the response is ruled by frictional behaviour in which the contribution of cohesion is neglected as suggested in [6]. In particular, a static friction coefficient  $\mu$  equal to 0.5 is assumed. In the normal direction, detachment is allowed with zero stiffness while an almost infinite stiffness  $k_n$  is assumed in compression to simulate a rigid normal contact. Tangential and normal behaviour are assumed uncoupled. The mechanical parameters adopted in the model are reported in Table 1.

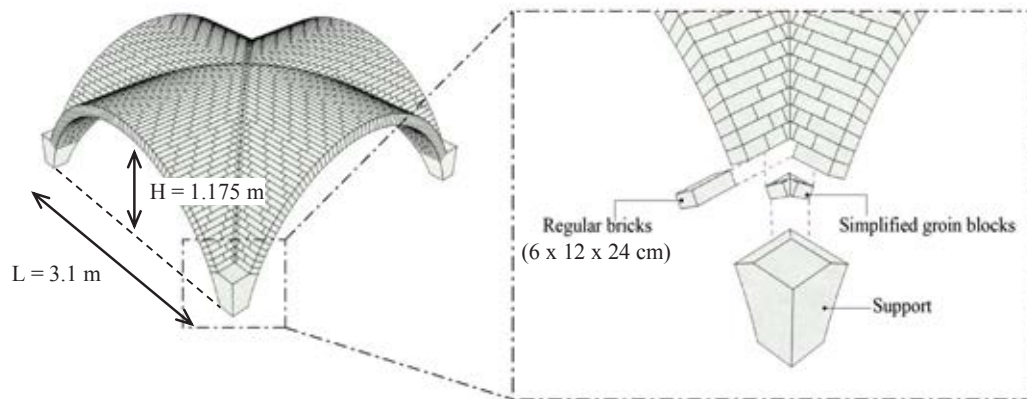


Figure 1: Geometry and discretization of the vault.

Blocks			Joints	
$\rho$ [kg/m <sup>3</sup> ]	$E$ [MPa]	$\nu$ [-]	$\mu$ [-]	$k_n$ [N/m <sup>3</sup> ]
1800	1200	0.2	0.5	$5 \cdot 10^9$

Table 1: Mechanical parameters.

## 2.2 Load conditions

The seismic performance of the cross vault is analysed through pushover analyses, by applying a monotonic lateral load to the structure. The analysis is divided in two steps: first the gravitational acceleration is applied, then the horizontal acceleration is applied. Two different inclinations of the horizontal acceleration are considered, i.e.,  $\theta = 0^\circ$  and  $\theta = 45^\circ$ , the angle  $\theta$  being defined in Figure 2. It is noted that, because of the symmetry of the model, there is no need to study both positive and negative directions.

The vault is confined by lateral Deformable Arches (DA) on three sides and by a rigid wall on one side (Figure 3). The boundary arches are 27 cm thick (i.e., about twice the vault thickness) and 50 cm depth. The mechanical properties adopted for the DAs are the same adopted for the masonry of the vault. Figure 3 also shows the fictitious plane which is introduced in the model to simulate the unilateral constraint of a rigid wall: the head arch of the vault in contact with the fictitious plane can detach from the plane, while it is prevented to compenetrare inside it. Similarly, contact between blocks of head arches and boundary structures is defined using the same interface behaviour adopted in the block-to-block contact definition. This means that normal compressive forces can arise, while no tension forces can develop.

Shear forces along the planes of the boundary structures can be generated, depending on the normal forces, according to the Mohr-Coulomb criterion.

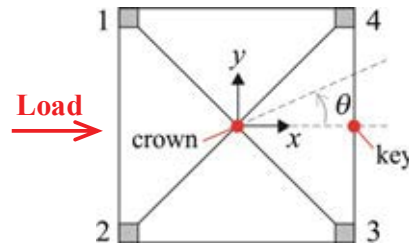


Figure 2: Push-over analysis: lateral load direction and control nodes.

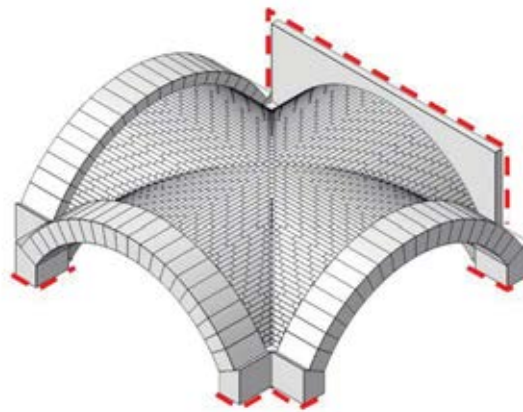


Figure 3: Boundary conditions. Pinned supports in red.

### 3 PARAMETRIC ANALYSIS

A parametric numerical study is conducted with the aim of highlighting the effect of the masonry apparatus. Table 2 reports the list of the performed simulations. The results will be commented in the following sections.

ID	Pattern	Confinement	Angle [°]
1	R	DA	0
2	D	DA	0
3	R	DA	45
4	D	DA	45

Table 2: Parametric analysis.

### 4 RESULTS

By looking at the deformed shapes in Figure 4, it is possible to notice that the two vaults behave quite differently. Note that the deformed shapes are plotted without boundary arches, with the exception of plan and axonometric views, to better highlight the collapse mechanism of the vaults. When  $\theta=0^\circ$ , the radial vault collapses due to the formation of a global mechanism characterized by four parallel hinges normal to the direction of the seismic action. On the contrary, the diagonal vault does not experience a global collapse, but only one cap under-

goes instability. When the angle of the seismic action is  $\theta=45^\circ$ , the deformed shapes show an almost symmetric collapse mechanism on both radial and diagonal vaults, with respect to groins, as visible in Figure 5. In particular, the radial vault shows the formation of parallel hinges along the bed joints, once again denoting a global collapse mechanism. However, a local failure occurs in the region along the groins, where the sliding and detachment of few bricks take place. The diagonal vault shows a quite different crack pattern in comparison to the radial vault and a local failure occurs at the head arches of two opposite caps.

Figure 6 plots the load-displacement curves in the case of horizontal acceleration along the  $x$ -axis direction ( $\theta=0^\circ$ ), for both considered masonry patterns. Two different control nodes have been chosen, in order to monitor the horizontal displacement in the  $x$ -direction: one node at the crown of the vault and one node at the key of the head arch of one cap, as shown in Figure 2. The load factor is obtained by normalizing the sum of the horizontal forces at the abutments to the vault's weight  $W$ , including the weight of the lateral confinement structures. The markers in Figure 6 and Figure 7 are referred to the values of imposed displacement  $u_{c,Crown}$  and  $u_{c,Key}$  that correspond to the activation of a failure mechanism.

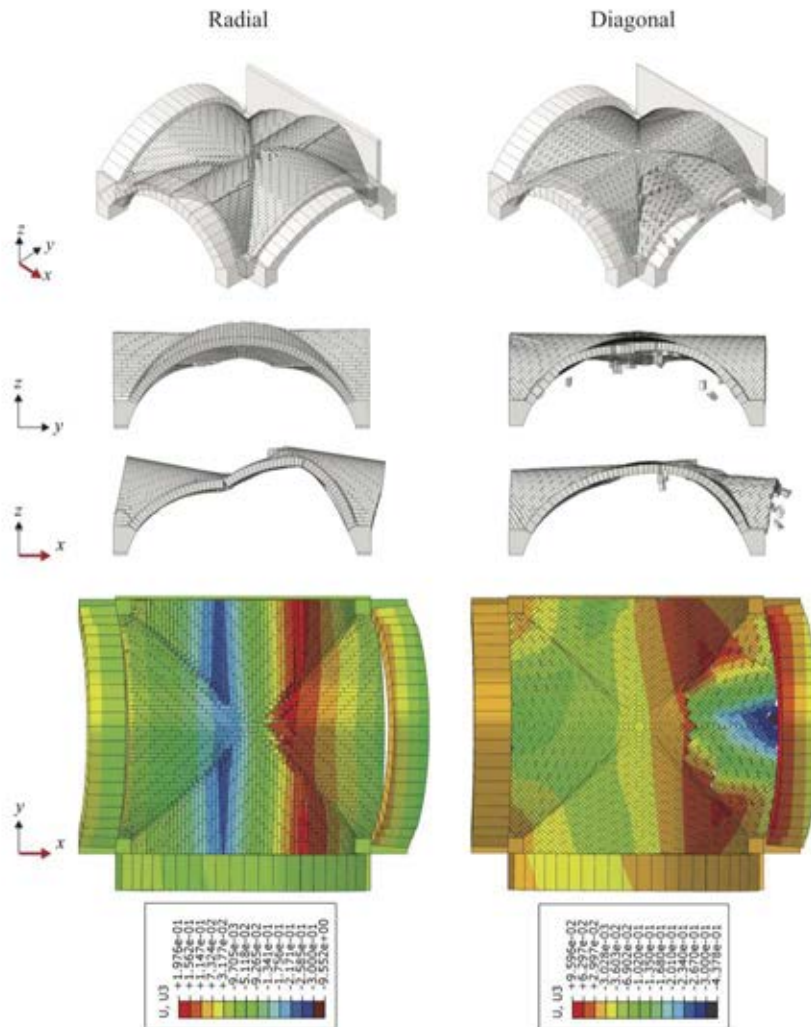


Figure 4: Collapse shapes in Pushover analysis for  $\theta = 0^\circ$ : axonometric view (first row),  $x$ - $z$  plane view (second row),  $y$ - $z$  plane view (third row), planar view with contour plot of  $u_z$  displacement [m] (fourth row).



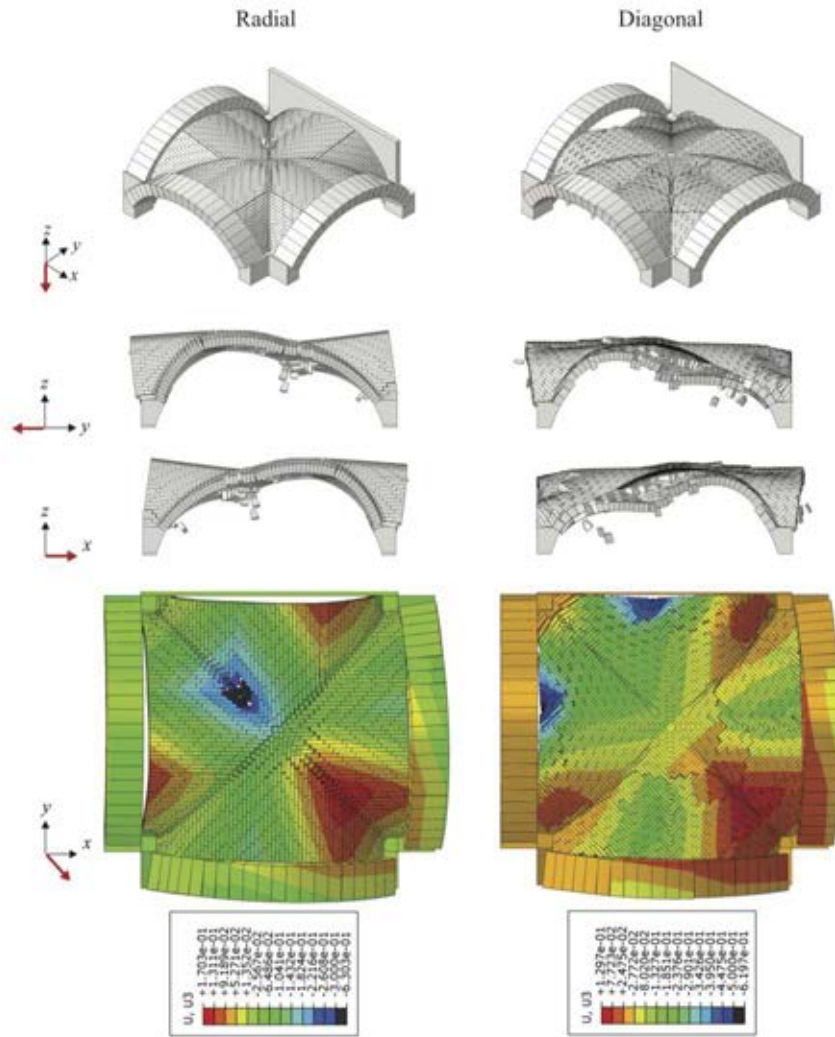


Figure 5: Collapse shapes in Pushover analysis for  $\theta=45^\circ$ : axonometric view (first row), y-z plane view (second row), x-z plane view (third row), planar view with contour plot of  $u_z$  displacement [m] (fourth row).

They have been identified by monitoring the reaction forces at each support, referring to a sudden decrease of force on the load-displacement curves, as visible in Figure 8.

In order to compare the capacity curves, the following quantities have been identified:

- $R_{\max}$ , peak value of the load factor;
- $u_{c,Crown}$ , maximum horizontal displacement at the crown of the vault before the activation of a collapse mechanism;
- $u_{c,Key}$ , maximum horizontal displacement at the key of one head arch before the activation of a collapse mechanism;
- $K_{el}$ , elastic stiffness, calculated as the ratio  $R_{60}/u_{60}$  between the 60% of  $R_{\max}$  and the corresponding settlement;
- $u_{80}/u_{60}$ , ductility parameter where  $u_{80}$  is the settlement corresponding to  $R_{80}$ , i.e., to a post-peak 20% reduction of  $R_{\max}$ .

Table 3 reports the values of the above-defined quantities, while Table 4 reports their variation with respect to the radial pattern case for  $\theta=0^\circ$ . In particular, the table reports the variations in terms of  $\Delta Q = (Q_{\text{pattern}} - Q_{\text{radial}})/Q_{\text{radial}} \cdot 100$ , where  $Q$  is the generic quantity.

It can be observed that the two vaults have quite similar capacity, with variations below 20% with respect to the radial configuration for  $\theta=0^\circ$ . Also their behaviour in terms of elastic stiffness is similar, whereas the values of ductility differs greatly, depending on the considered pattern and value of  $\theta$ . Specifically, when  $\theta=0^\circ$  the diagonal vault is the one characterized by the lowest elastic stiffness (14.52% lower than the radial vault) and by the highest reduction of ductility with respect to the radial pattern (-53.08%). This last aspect is also visible in the load displacement curves in Figure 6, by looking at the values of displacement of the control nodes. As a matter of fact, in the radial vault, the horizontal displacement of the head arch is only 1.16 times greater than the horizontal displacement of the crown of the vault, whereas in the diagonal vault it is 2.65 times greater.

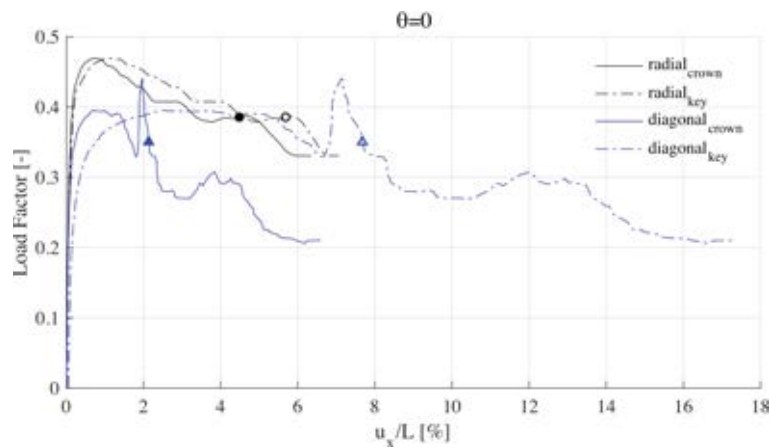


Figure 6: Capacity curves of confined radial and diagonal cross vaults for  $\theta=0^\circ$ .

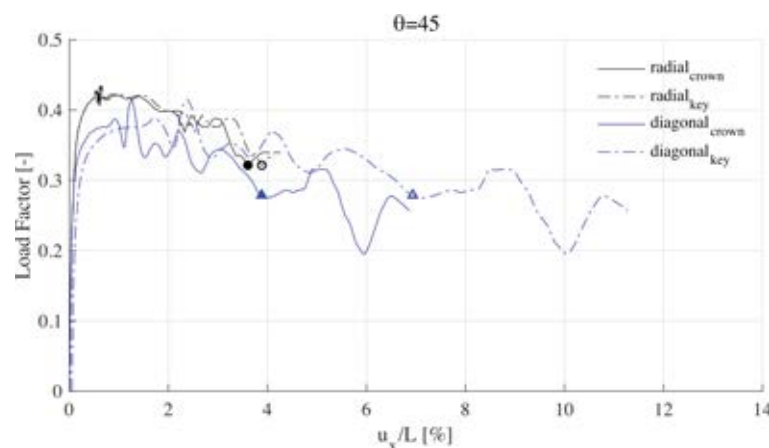
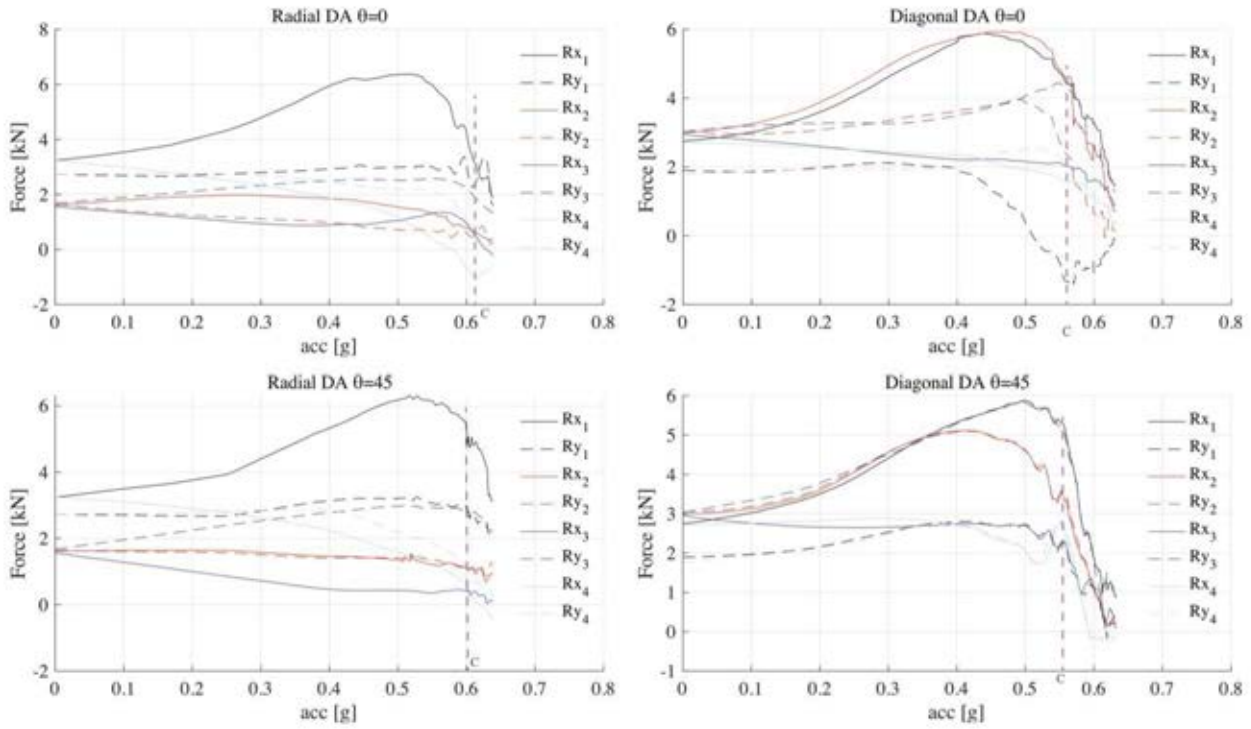


Figure 7: Capacity curves of confined radial and diagonal cross vaults for  $\theta=45^\circ$ .

Figure 8: Reaction forces  $R_x$  and  $R_y$  at the abutments vs. horizontal acceleration.

This means that the diagonal vault undergoes a partial collapse of one cap, but the crown of the vault is still stable. The different deformation mechanism induced by the two brick laying techniques is also highlighted by the vertical displacement field of the vaults, plotted before the activation of a collapse mechanism. In the case of the diagonal vault it is clearly visible how the damage is concentrated mostly in one cap, while the rest of the structure results almost undamaged.

When the direction of the seismic action is parallel to the groins, hence for  $\theta=45^\circ$ , the vault arranged with the diagonal pattern provides the greatest increase of ductility (+31.67%), while the radial vault suffers a decrease of ductility of about 8.84% if compared to the same vault with  $\theta=0^\circ$ . The radial vault also experiences the greatest increase of elastic stiffness, being 20.61% greater than the loading condition with  $\theta=0^\circ$ .

Pattern	$R_{\max}$ [-]	$u_{c,Crown}$ [m]	$u_{c,Key}$ [m]	$R_{60}$ [-]	$u_{60,Crown}$ [m]	$K_{el}$ [N/m]·10 <sup>6</sup>	$u_{80,Crown}$ [m]	$u_{80} / u_{60}$ [-]
Radial $\theta=0^\circ$	0.469	0.131	0.169	0.282	0.0020	10.05	0.158	78.9
Diagonal $\theta=0^\circ$	0.394	0.064	0.233	0.236	0.0019	8.59	0.072	37.02
Radial $\theta=45^\circ$	0.419	0.109	0.118	0.251	0.0015	12.12	0.107	71.94
Diagonal $\theta=45^\circ$	0.374	0.118	0.211	0.225	0.0014	11.07	0.150	68.45

Table 3: Critical quantities used for comparison between brick patterns.



Pattern	$\Delta R_{\max}$ [%]	$\Delta K_{el}$ [%]	$\Delta(u_{80} / u_{60})$ [%]
Diagonal $\theta = 0^\circ$	-16.07	-14.52	-53.08
Radial $\theta = 45^\circ$	-10.68	20.61	-8.84
Diagonal $\theta = 45^\circ$	-20.22	10.21	31.67

Table 4: Variation of peak reaction force, elastic stiffness and ductility compared to the radial vault with  $\theta = 0^\circ$ .

## 5 CONCLUSIONS

- In this paper the results of a parametric analysis on the seismic response of cross masonry vaults are presented.
- The geometry of an ideal vault is considered taking into account its detailed brick pattern.
- The FEM simplified micro-modelling approach is adopted for the discretization of the volume of the structure, endowing the interfaces with tangential frictional behaviour and normal rigid compressive contact. Free detachment is allowed under traction. Linear elastic behaviour is assumed for the masonry blocks.
- Two different brick patterns are considered, i.e., radial and diagonal. Static non-linear analyses are performed, assuming two different directions of the seismic input in the horizontal plane, namely  $0^\circ$  and  $45^\circ$ .
- The results show that the influence of the brick pattern on the seismic response is limited in terms of seismic load capacity and elastic stiffness, while it highly affects the ductility. In particular, diagonal bed joints are able to provide the vault with almost twice displacement capacity.

## REFERENCES

- [1] P.B. Lourenco, J.G. Rots, J. Blaauwendraad, Two approaches for the analysis of masonry structures - micro and macro-modeling. *HERON*, **40**(4), 313-340, 1995.
- [2] M. Alforno, A. Monaco, F. Venuti, C. Calderini. Validation of simplified micro-models for the static analysis of masonry arches and vaults. *International Journal of Architectural Heritage*, 1-17, 2020.
- [3] M. Rossi, C. Calderini, S. Lagomarsino. Experimental testing of the seismic in-plane displacement capacity of masonry cross vaults through a scale model. *Bulletin of Earthquake Engineering*, **14**, 261-281, 2016.
- [4] M. Alforno, F. Venuti, A. Monaco. The structural effects of micro-geometry on masonry vaults. *Nexus Network Journal*, **22**, 1237–1258, 2020.
- [5] M. Alforno, C. Calderini, A. Monaco, F. Venuti, Numerical modelling of masonry vaults with different brick pattern. *IASS Annual Symposium 2019 – Structural Membranes 2019 – Form and Force*, Barcelona, Spain, October 7-10, 2019.

- [6] A.M. D’Altri, V. Sarhosis, G. Milani, J. Rots, S. Cattari, S. Lagomarsino, E. Sacco, A. Tralli, G. Castellazzi, S. de Miranda. Modeling Strategies for the Computational Analysis of Unreinforced Masonry Structures: Review and Classification. *Archives of Computational Methods in Engineering*, **27**, 1153–1185, 2020.